Theor Chim Acta (1991) 81: 105–123

Theoretica Chimica Acta

Analysis of the π-electronic structure of infinitely large networks

IV. Polycyclic aromatics with bond alternation

Ying-Duo Gao and Haruo Hosoya

Department of Chemistry, Ochanomizu University, Bunkyo-ku, Tokyo 112, Japan

Received February 20, 1990/Received in revised form and accepted February 18, 1991

Summary. Applying the Coulson and Longuet-Higgins integral method to polycyclic aromatics, the analytical solutions of bond orders, π-electronic energy and benzene character for the infinitely large cyclic polyacene and polyphenanthrene with various modes of bond alternation are obtained in the HMO scheme. Most of the results are explicitly and newly expressed in terms of three kinds of the elliptic integrals. Judging from the magnitudes of bond orders and benzene character the most probable modes of the bond alternation for these two networks are discussed with their Kekulé structures. It was shown that if bond alternation is properly taken into consideration, HMO calculation can fairly well reproduce the results obtained by more sophisticated methods.

Key words: Coulson's integral method – Bond alternation – π-Electronic structure – Polycyclic aromatics

1. Introduction

Search for organic conductors of polycyclic aromatic hydrocarbons has long been pursued. Among the possible candidates, the electronic structure of the simplest one, polyacene, and its structural isomer, polyphenanthrene, has been studied by many researchers [1–15], although they have not been synthesized yet. The discussions have been focused on energetic stability, band structure and bond alternation.

Although among the existing MO theories the Hückel MO method is the simplest, its most advantageous point is that it can afford analytical expressions of important electronic properties within its scheme, especially for infinitely large networks. If we are concerned only with alternant hydrocarbons, either acyclic or aromatic, its semiqualitative predictability have been found to increase with the size of molecules by properly taking into account the bond alternation parameters, if necessary. As will be shown later in this paper, the bond order pattern obtained in this line reproduces remarkably well that of more sophisticated methods. The relative magnitudes of HOMO-LUMO gap obtained by HMO have also shown to be linearly related to those predicted by the elaborated calculation [16].

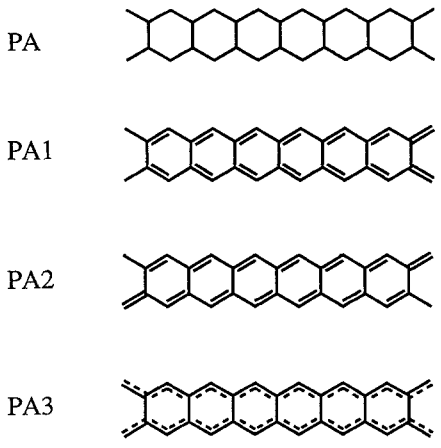

Fig. 1. Structure and isometric patterns of polyacene

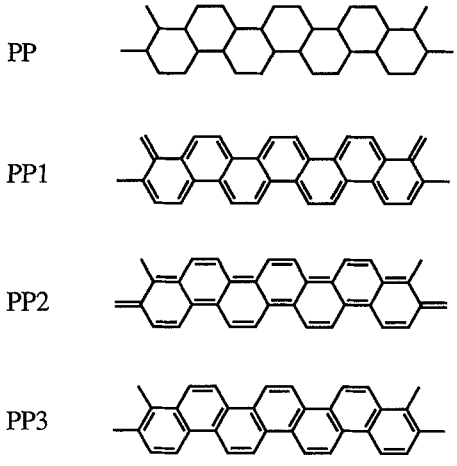

Fig. 2. Structure and isometric patterns of polyphenanthrene

The purpose of the present work is to present the analytical expressions for the results of various HMO properties for the infinitely large polymer networks of polyacene (PA) (Fig. 1) and polyphenanthrene (PP) (Fig. 2) by modifying the Coulson and Longuet-Higgins integral method [17] and also to clarify the mathematical structure in the topological dependency of the π-electronic properties of periodic lattices. Although for the former network a number of studies have been reported, for the latter only a few systematic treatments have been performed. We could obtain a series of useful analytical results which can be used for refining the argument of more sophisticated theories [18, 19]. The capability and limitation of the analytical HMO method with bond alternation are also discussed.

2. Application of the Coulson and Longuet-Higgins method to linear polycyclic systems

Coulson and Longuet-Higgins [17] found that the π-electronic energy, E_π, of the closed-shell ground-state of a conjugated unsaturated hydrocarbon molecule G with N electrons is expressed by:

$$E_\pi = 2\sum_{n=1}^{[N/2]} x_n = \frac{1}{\pi}\int_{-\infty}^{\infty}\left[\frac{iy\,\Delta'_G(iy)}{P_G(iy)} - N\right]dy, \tag{1}$$

where γ is an infinitely large semicircle in the complex plane, Δ'_G is the first derivative of the secular polynomial Δ_G, or P_G, the characteristic polynomial:

$$P_G(x) = \sum_{k=0}^{N} a_k x^{N-k}, \tag{2}$$

which is derived by expanding the secular determinant $|\mathbb{A} - x\mathbb{E}|$ constructed from the adjacency matrix $\mathbb{A}$ of G and the unit matrix $\mathbb{E}$.

The Coulson's bond order in G is obtained by the following expression:

$$\begin{aligned} p_{rs} &= -\frac{1}{i\pi}\oint_\gamma \frac{\Delta_{rs}(z)}{P_G(z)}\,dz \\ &= (-1)^{r+s+1}\frac{1}{\pi}\int_{-\infty}^{\infty}\frac{\Delta_{rs}(iy)}{P_G(iy)}\,dy. \end{aligned} \tag{3}$$

In order to perform the integration for an infinitely large periodic system, we have employed two different tactics previously [18, 19], namely the use of recursive relations and double integration involving k vectors. In the present work, the latter method is adopted. The bond order can be expressed as:

$$p_{rs} = (-1)^{r+s+1}\frac{1}{2\pi^2}\int_0^{2\pi}\int_{-\infty}^{\infty}\frac{\Delta_{k,rs}(iy)}{\Delta_k(iy)}\,dy\,dk\,\theta, \tag{4}$$

where Δ_k is the k-th determinant factored out from Δ_G (or P_G) as will be exemplified in the next section, and $\Delta_{k,rs}$ is obtained by deleting the r-th row and s-th column from Δ_k.

3. Polyacene

For infinitely large polyacene, since much has already been discussed [1–15], the method for performing the complex integral will briefly be mentioned in the following. For this network, we first assume that there are three types of C–C bonds as shown in Fig. 3(a) (C_{2v} structure), where a_1, a_2 and a_3 are bond alternation parameters, denoting the ratios of the resonance integrals to that of the "purely double bond". The polymer can be constructed from butadiene units as shown in Chart 1(a), where the numbering of atoms is also given [20]. Then according to the periodic boundary condition, we obtain the characteristic polynomial as:

$$P_G(x) = \Delta_G(x) = \prod_{k=1}^{N}\Delta_k(x), \tag{5}$$

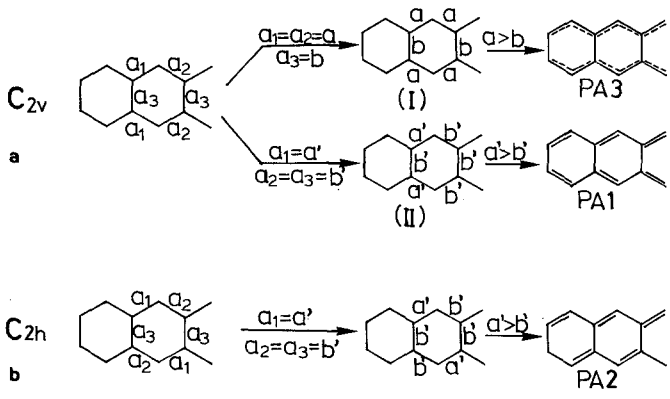

Fig. 3. Relation among various patterns of PA with different sets of bond alternation parameters

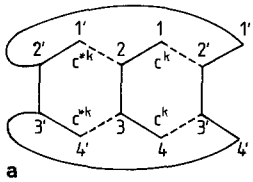

Chart 1(a)

where

$$\Delta_k(x) = \begin{vmatrix} -x & a_1 + a_2 c^k & 0 & 0 \\ a_1 + a_2 c^{*k} & -x & a_3 & 0 \\ 0 & a_3 & -x & a_1 + a_2 c^{*k} \\ 0 & 0 & a_1 + a_2 c^k & -x \end{vmatrix}$$

$$= x^4 - (a_3^2 + 2a_1^2 + 2a_2^2 + 4a_1 a_2 \cos k\theta)x^2 + (a_1^2 + a_2^2 + 2a_1 a_2 \cos k\theta)^2, \quad (6)$$

with $c = \exp(i\theta)$ and $c^* = \exp(-i\theta)$, $(\theta = 2\pi/N)$. Note that for large N, the argument $k\theta$ can be deemed as a continuously changing variable in the range of $0 \leqslant k\theta \leqslant 2\pi$.

For bond 1,2; 2,3; 1,4 and 1′2, we have:

$$\Delta_{k,12}(x) = -(a_1 + a_2 \cos k\theta)[x^2 - (a_1^2 + a_2^2 + 2a_1 a_2 \cos k\theta)], \quad (7)$$

$$\Delta_{k,23}(x) = -a_3 x^2, \quad (8)$$

$$\Delta_{k,14}(x) = -a_3(a_1^2 + a_2^2 + 2a_1 a_2 \cos k\theta), \quad (9)$$

and

$$\Delta_{k,1'2}(x) = -(a_2 + a_1 \cos k\theta)[x^2 - (a_1^2 + a_2^2 + 2a_1 2a_2 \cos k\theta)]. \quad (10)$$

By using Eq. (4), we can derive the bond order p_{12} as follows:

$$p_{12} = \frac{2}{\pi^2}\int_0^{\pi}\int_0^{\infty} \frac{\Delta_{k,12}(ix)}{\Delta_k(ix)}\,dx\,dk\,\theta$$

$$= \frac{1}{\pi}\int_0^{\pi} \frac{2(a_1 + a_2\cos k\theta)}{\sqrt{a_3^2 + 4(a_1^2 + a_2^2) + 8a_1a_2\cos k\theta}}\,dk\,\theta$$

$$= \frac{4a_1^2 - (a_3^2 + 4a_2^2)}{2\pi a_1\sqrt{a_3^2 + 4(a_1 + a_2)^2}}\,K\left(\sqrt{\frac{16a_1a_2}{a_3^2 + 4(a_1 + a_2)^2}}\right)$$

$$+ \frac{\sqrt{a_3^2 + 4(a_1 + a_2)^2}}{2\pi a_1}\,E\left(\sqrt{\frac{16a_1a_2}{a_3^2 + 4(a_1 + a_2)^2}}\right), \tag{11}$$

where K and E are the first and second kinds of the complete elliptic integrals, respectively [21]:

$$K(k) = \int_0^{\pi/2} \frac{d\theta}{\sqrt{1 - k^2\sin^2\theta}}, \tag{12}$$

$$E(k) = \int_0^{\pi/2} \sqrt{1 - k^2\sin^2\theta}\,d\theta. \tag{13}$$

Similarly, for bonds 2,3; 1,4 and 1′2, the analytical expressions are obtained as:

$$p_{23} = \frac{2a_3}{\pi\sqrt{a_3^2 + 4(a_1 + a_2)^2}}\,K\left(\sqrt{\frac{16a_1a_2}{a_3^2 + 4(a_1 + a_2)^2}}\right) = -p_{14}. \tag{14}$$

$$p_{1'2} = \frac{4a_2^2 - (a_3^2 + 4a_1^2)}{2\pi a_2\sqrt{a_3^2 + 4(a_1 + a_2)^2}}\,K\left(\sqrt{\frac{16a_1a_2}{a_3^2 + 4(a_1 + a_2)^2}}\right)$$

$$+ \frac{\sqrt{a_3^2 + 4(a_1 + a_2)^2}}{2\pi a_2}\,E\left(\sqrt{\frac{16a_1a_2}{a_3^2 + 4(a_1 + a_2)^2}}\right). \tag{15}$$

Since the zeros of $P_G(x)$ for PA are given by:

$$x = \pm\tfrac{1}{2}\left(\sqrt{a_3^2 + 4(a_1^2 + a_2^2) + 8a_1a_2\cos k\theta} \pm a_3\right), \tag{16}$$

we can obtain the energy per π-electron as:

$$\bar{\varepsilon}_\pi = \frac{\sqrt{a_3^2 + 4(a_1 + a_2)^2}}{\pi}\,E\left(\sqrt{\frac{16a_1a_2}{a_3^2 + 4(a_1 + a_2)^2}}\right). \tag{17}$$

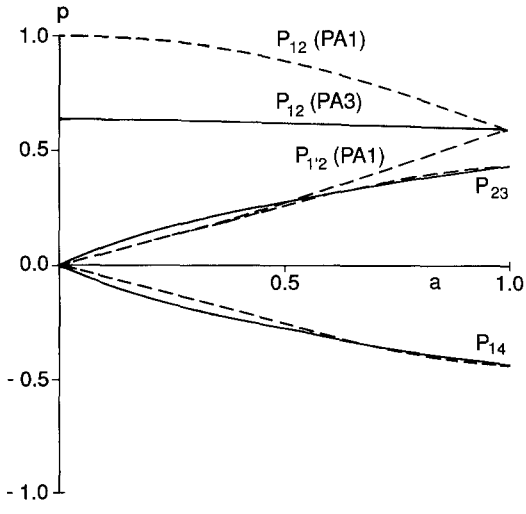

Fig. 4. Curves of the bond orders as a function of bond alternation parameter a. The *dashed* and *solid lines* are those for PA1 and PA3, respectively

It should be noted that, the relation between the bond orders and the π-electronic energy is obtained to be:

$$\bar{\varepsilon}_\pi = \tfrac{1}{2}(2a_1 p_{12} + 2a_2 p_{1'2} + a_3 p_{23}), \tag{18}$$

as expected from the scheme of the tight-binding approximation.

It is obvious that, in a particular case of $a_1 = 1$ and $a_2 = a_3 = a \neq 1$, the polymer has the bond alternation pattern PA1 as shown in Fig. 1, and that when $a_1 = a_2 = 1$ and $a_3 = a \neq 1$, the polymer becomes PA3. The bond orders, p_{12}, p_{23}, p_{14}, and $p_{1'2}$, of PA1 and PA3 as a function of bond alternation parameter a are plotted in Fig. 4 by the dashed and solid lines, respectively. The value of p_{12} for PA3 with $a = 0$ is 0.636620, which is the same as that for polyacetylene with no bond alternation [18]. The p_{23} and p_{14} ($= -p_{23}$) for PA3 are found to have no large difference from those of PA1.

Bond alternation may occur in another way as shown in PA2 in Fig. 1 or Fig. 3b, where bond alternation pattern in the two polyacetylene-like chains have C_{2h} symmetry. In this case, the factor $\Delta_k(x)$ of the characteristic polynomial is given as:

$$\Delta_k(x) = \begin{vmatrix} -x & a_1 + a_2 c^k & 0 & 0 \\ a_1 + a_2 c^{*k} & -x & a_3 & 0 \\ 0 & a_3 & -x & a_2 + a_1 c^{*k} \\ 0 & 0 & a_2 + a_1 c^k & -x \end{vmatrix}$$

$$= x^4 - (a_3^2 + 2a_1^2 + 2a_2^2 + 4a_1 a_2 \cos k\theta)x^2 + (a_1^2 + a_2^2 + 2a_1 a_2 \cos k\theta)^2, \tag{19}$$

which turns out to be the same as Eq. (6). Similarly we find that $\Delta_{k,12}(x)$ and $\Delta_{k,23}(x)$ are also the same as Eqs. (7) and (8), and $\Delta_{k,34}(x)$ are identical with Eq. (10), so in this case the bond orders, p_{12}, p_{23}, and p_{34}, have the same expressions as those of PA1 of Fig. 1.

However, the bond order p_{14} is a little bit complicated as:

$$p_{14} = \frac{-a_3}{\pi a_1 a_2 \sqrt{a_3^2 + 4(a_1 + a_2)^2}} \left\{ (a_1^2 + a_2^2) K \left(\sqrt{\frac{16 a_1 a_2}{a_3^2 + 4(a_1 + a_2)^2}} \right) \right.$$

$$\left. - (a_1 - a_2)^2 \Pi \left(\frac{4 a_1 a_2}{(a_1 + a_2)^2}, \sqrt{\frac{16 a_1 a_2}{a_3^2 + 4(a_1 + a_2)^2}} \right) \right\}, \tag{20}$$

where Π is the third kind complete elliptic integral:

$$\Pi(c, k) = \int_0^{\pi/2} \frac{d\theta}{(1 + c \sin^2 \theta) \sqrt{1 - k^2 \sin^2 \theta}}. \tag{21}$$

When $a_1 = 1, a_2 = a_3 = a \neq 1$, the polymer has the bond alternation pattern PA2 as in Fig. 1. Since Eq. (19) is the same as Eq. (6), the energy per π-electron of PA2 should be equal to that of PA1 as long as the same set of bond alternation parameters is chosen.

As mentioned above, we only considered the three simplest cases, namely, PA1, PA2 and PA3. In the following discussion, let us confine ourselves to the two cases which involves two parameters.

If we let $a_1 = a_2 = a$ and $a_3 = b$, pattern I is obtained (see Fig. 3). Note that PA3 is the case with $a > b$. If we let $a_1 = a'$ and $a_2 = a_3 = b'$, pattern II is obtained. PA1 is the case with $a' > b'$. By changing parameters a, b, a' and b', one can get more information on the effect of bond alternation than the simple plots of Fig. 4. We could find that by choosing the parameters as $a = 0.83$ and $b = 0.76$ for pattern II, the bond order of p_{12}, $p_{1'2}$ and p_{23}, are obtained, respectively, to be 0.646, 0.543 and 0.422, which are compatible with the values of 0.650, 0.547 and 0.405, obtained by more sophisticated calculation, the so-called one-dimensional tight-binding SCF-CO (crystal orbital) method [4].

Figure 5a shows the dependency of $\bar{\varepsilon}_\pi$ on b and b' with certain fixed values of a and a' (1.0, 0.9, 0.8 and 0.6). These curves were calculated from Eq. (17). If we use the same values for the parameters as $a = a'$ and $b = b'$ in pattern I and II, pattern I becomes more stable than pattern II in all the range of $0 \leqslant b \leqslant a$. Similar curves of $\bar{\varepsilon}_\pi$ can be drawn as Fig. 5b for the $a(a')$-dependency with fixed values of $b(b')$. However, within this model we cannot determine which pattern is more stable unless the values of parameters a, a', b, and b' are specified from other reasoning. Nevertheless, the results obtained here could provide us ample information on the effect of bond alternation to the electronic structures of their networks.

We can calculate the band structures of these isomers [20] as a function of parameter a as shown in Fig. 6, where the right half is that of PA3, and the left half is for PA1 and PA2. Toward $a = 1$, both the curves become identical. The band structure of PA1 and PA2 are obtained from Eq. (16) with $a_1 = 1$ and $a_2 = a_3 = a$. More general feature of the band structure involving three parameters is shown in Fig. 7, where the unoccupied part is omitted as it is symmetrical with the occupied part. The condition for the two bands to overlap is:

$$\frac{2}{a_3} > \sqrt{\frac{1}{a_1^2} + \frac{1}{a_2^2}}. \tag{22}$$

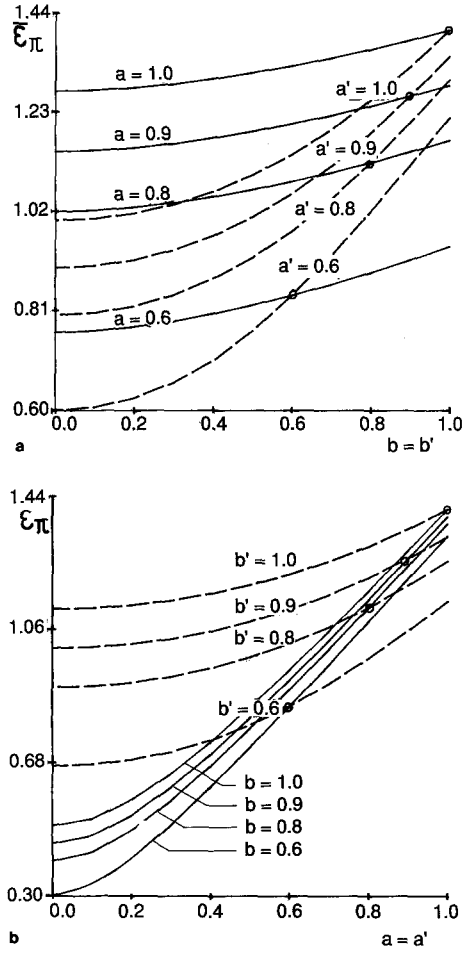

Fig. 5. **a** Curves of the energy per π-electron, $\bar{\varepsilon}_\pi$, as a function of parameter b for several a and a' values. The *solid* and *dashed lines* are for patterns I and II respectively. **b** The curves of the energy per π-electron, $\bar{\varepsilon}_\pi$, as a function of parameter a for several b and b' values. The *solid* and *dashed lines* are for patterns I and II, respectively

Clearly, Eq. (22) is satisfied for PA1 and PA2 since $a_1 = 1$, and for PA3 since $a_1 = a_2 = 1$, so that the two bands overlap with each other in Fig. 6, respectively. Figure 7 implicitly contains the results of Salem and Longuet-Higgins [1].

For PA3 as seen from Fig. 6, no HOMO-LUMO band gap is expected no matter what the bond alternation parameter is. It implies that in this model, the polymer of PA3 pattern will never have a gap at the Fermi level. Since PA3 can be considered as to be constructed from two polyacetylene chains without bond alternation, the property of the π-electronic structure of PA3 is basically identical with that of polyacetylene. The bridge bonds connecting the two chains do not change the character of the Fermi level at all. On the other hand, for PA1 when bond alternation is introduced, a band gap opens up at the Fermi level as has been pointed out by several authors [1–4]. However, an important point to

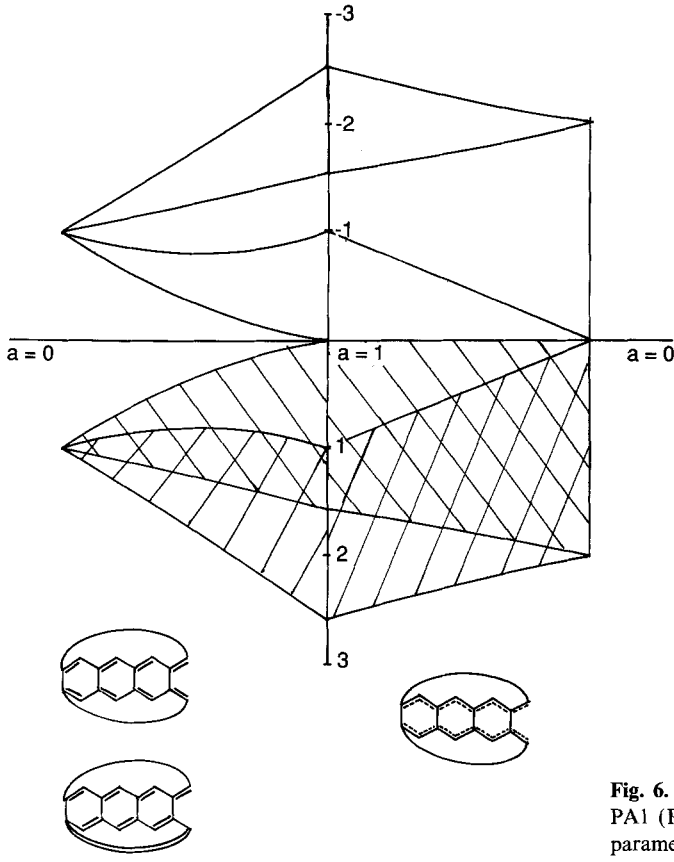

Fig. 6. Band structures of PA1 (PA2) and PA3 versus parameter a

$$x = \pm \frac{1}{2}\left[\sqrt{a_3^2 + 4(a_1^2 + a_2^2 + 2a_1a_2\cos k\theta)} \pm a_3\right]$$

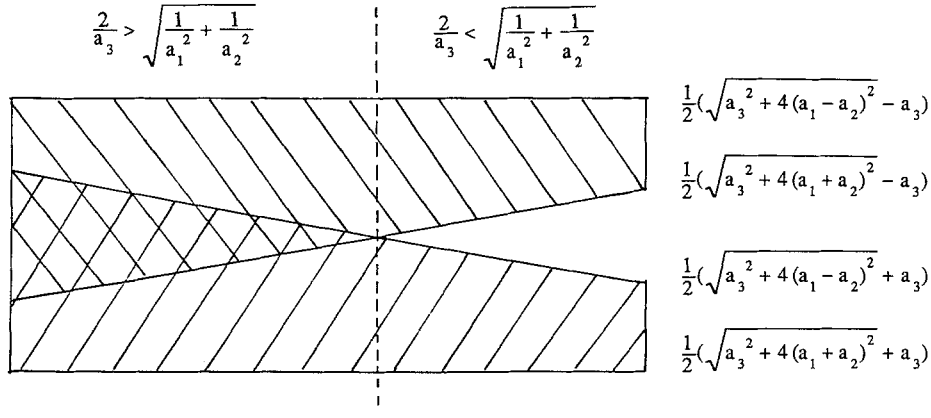

Fig. 7. Schematic diagram of band structure for polyacene with bond alternation

be noted is that, the occurrence of the band gap for PA1 does not mean that the bond alternation stabilizes PA1 relative to PA3 (Peierls transition), as reflected in the $\bar{\varepsilon}_\pi$ for these structures (see Fig. 5).

The density of states, dk/dx, of these structures can also be drawn by using the analytical expressions as Eq. (16) [20, 22] for a given set of bond alternation parameters (a_1, a_2, a_3).

Although Eqs. (2.5) and (4.3) of Ref. [1] by Salem and Longuet-Higgins implicitly contain some of our results of energy per π-electron and bond orders, the physical meaning of the results has not been discussed in detail by them. Moreover, the bond order of bond 1,4, namely the *para* bond in a benzene ring, cannot be calculated by the method proposed in Ref. [1]. As will be clear in Sect. 5 of this work, the bond order of the *para* bond is necessary for calculating the benzene character of a given aromatic hydrocarbon. In this sense our method is better suited for analyzing the property of aromatics.

4. Polyphenanthrene

For the infinitely large polyphenanthrene (PP), the analytical solutions of bond orders and π-electronic energy have never been obtained yet. Since the method of derivation is analogous to that of PA, in the following, we only give the analytical results of these physical properties.

In the PP network, there should be three types of C–C bonds as considered for PA, however, the analytical results could not be obtained if three parameters are introduced. We therefore assume three types of bond alternation pattern as shown in Fig. 2 instead of treating the calculation involving three parameters. The resonance integral of the single and double bonds are assigned as β_s and β_d, respectively, and the bond alternation parameter is defined as $a = \beta_s/\beta_d$.

As shown in Chart 1(b), polyphenanthrene can also be constructed from butadiene units in a different mode from polyacene [20].

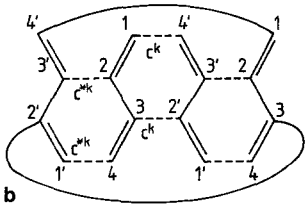

b

Chart 1(b)

The factor of the characteristic polynomial for PP1 can be expressed as:

$$\Delta_k(x) = \begin{vmatrix} -x & 1 & 0 & ac^k \\ 1 & -x & a(1+c^{*k}) & 0 \\ 0 & a(1+c^k) & -x & 1 \\ ac^{*k} & 0 & 1 & -x \end{vmatrix}$$

$$= x^4 - x^2(3a^2 + 2 + 2a^2 \cos k\theta) + [2a^4(1 + \cos k\theta) - 2a^2(2\cos^2 k\theta + \cos k\theta - 1) + 1]. \quad (23)$$

By using the similar method for PA, we can obtain the analytical solution for each bond. For example, for PP1 the bond order p_{12} is:

$$p_{12}=\frac{1}{2\pi\sqrt{a^2+4}}\left[(a\sqrt{a^2+4}+2-a^2)E\left(\frac{2\sqrt{2a(\sqrt{a^2+4}-a)}}{a\sqrt{a^2+4}+2-a^2}\right)\right.$$
$$-(a\sqrt{a^2+4}-2-a^2)K\left(\frac{2\sqrt{2a(\sqrt{a^2+4}-a)}}{a\sqrt{a^2+4}+2-a^2}\right)$$
$$+(a\sqrt{a^2+4}+2+a^2)E\left(\frac{2\sqrt{2a(\sqrt{a^2+4}+a)}}{a\sqrt{a^2+4}+2+a^2}\right)$$
$$\left.-(a\sqrt{a^2+4}-2+a^2)K\left(\frac{2\sqrt{2a(\sqrt{a^2+4}+a)}}{a\sqrt{a^2+4}+2+a^2}\right)\right], \quad (24)$$

which can be expressed as:

$$p_{12}=[A_1E(k_1)+A_2E(k_2)]-[B_1K(k_1)+B_2K(k_2)], \quad (25)$$

where A_1, A_2, B_1, and B_2 are the coefficients of each term in (24), respectively.

Similarly, the analytical expressions for other bonds and energy per π-electron are obtained as summarized in Table 1.

Table 1. The coefficients in front of $E(k_1)$, $K(k_1)$, $E(k_2)$ and $K(k_2)$ in the expressions of bond orders p_{12}, p_{23}, p_{14}, p_{45}, p_{27}, p_{25} and p_{36} for PP1. The expression of energy per π-electron $\bar{\varepsilon}_k$ is also shown

p_{12}	A_1	$-B_1$	A_2	$-B_2$
p_{23}	CA_1	$-CB_1$	$-DA_2$	DB_2
p_{14}	DA_1	$-DB_1$	$-CA_2$	CB_2
p_{45}	$\frac{1}{a}[A_1$	B_1	A_2	$B_2]$
p_{27}	$\frac{1}{4a^2}[C^2A_1$	C^2B_1	D^2A_2	$D^2B_2]$
p_{25}	$\frac{1}{a}[CA_1$	CB_1	$-DA_2$	$-DB_2]$
p_{36}	$\frac{1}{3a^2}[(C^2-2a^2)A_1$	$(C^2+2a^2)B_1$	$(D^2-2a^2)A_2$	$(D^2+2a^2)B_2]$

$$\bar{\varepsilon}_\pi=\frac{1}{\pi}[(C+a)E(k_1)+CE(k_2)]=\tfrac{1}{2}(2p_{12}+ap_{23}+ap_{45}+ap_{27})$$

$$A_1=a\sqrt{a^2+4}+2-a^2, \qquad A_2=a\sqrt{a^2+4}+2+a^2$$

$$B_1=a\sqrt{a^2+4}-2-a^2, \qquad B_2=a\sqrt{a^2+4}-2+a^2$$

$$C=\frac{\sqrt{a^2+4}+a}{2}, \qquad D=\frac{\sqrt{a^2+4}-a}{2}$$

$$k_1=\frac{2\sqrt{2a(\sqrt{a^2+4}+a)}}{a\sqrt{a^2+4}+2+a^2}, \qquad k_2=\frac{2\sqrt{2a(\sqrt{a^2+4}-a)}}{a\sqrt{a^2+4}+2-a^2}$$

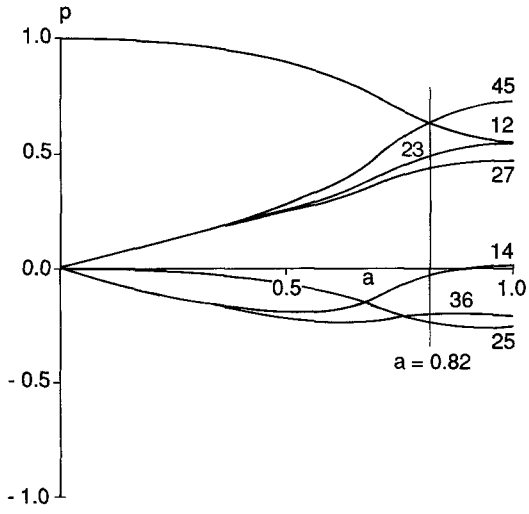

Fig. 8. Curves of the bond orders as a function of parameter a for PP1

The bond orders p_{12}, p_{23}, p_{14}, p_{45}, p_{27}, p_{25}, and p_{36} of PP1 are shown in Fig. 8 as a function of bond alternation parameter a. In the region with $0.98 < a < 1$, the principal bond orders are in the following order, $p_{45} > p_{23} > p_{12}$, which is in contradiction with the bond alternation pattern of PP1 in Fig. 2. The curve of p_{12} crosses with those of p_{45} and p_{23} at about $a = 0.82$ and 0.98, respectively. So, only when $a < 0.82$, these calculated bond orders are consistent with the pattern of PP1. The bond order for a pair of atoms belonging to the same class (starred or unstarred) is zero from the pairing theorem, while that for a pair of disjoint atoms but of different classes, such as para bond, plays an important role in the benzene character. Although the bond orders of those pairs of atoms show interesting behavior, for example, to give crossing points as can be seen from Fig. 8, no further discussion has been made.

Similarly for PP2, the analytical solutions of various bond orders and energy per π-electron are also obtained and shown in Table 2, which coincides with Table 1 for the special case with $a = 1$.

The curves of bond orders p_{12}, p_{23}, p_{14}, p_{45}, p_{27}, p_{25}, and p_{36} for PP2 are plotted in Fig. 9 as a function of the bond alternation parameter a. In the range of $0 \leqslant a \leqslant 1$, we can see the following order, $p_{45} > p_{23} > p_{12}$, is consistent with the pattern of PP2, but when $a > 0.9$, the bond order p_{27}, corresponding to a double bond, is smaller than p_{12} and p_{23}, those of the single bonds. Thus, similarly to the case of PP1, there is a certain range where the relative values of the bond orders are in contradiction with the bond alternation pattern of PP2 in Fig. 2. Since the value range of PP2 is wider than that of PP1, PP2 seems to be more plausible than PP1 in this respect.

For PP3, the factor $\Delta_k(x)$ of the characteristic polynomial is:

$$\Delta_k(x) = \begin{vmatrix} -x & a & 0 & c^k \\ a & -x & 1+ac^{*k} & 0 \\ 0 & 1+ac^k & -x & a \\ c^{*k} & 0 & a & -x \end{vmatrix}$$

$$= x^4 - (3a^2 + 2 + 2a\cos k\theta)x^2 + [-4a^3\cos^2 k\theta - 2a(a-1)\cos k\theta + a^2(a+1)^2 + 1]. \quad (26)$$

Table 2. The coefficients in front of $E(k_1)$, $K(k_1)$, $E(k_2)$ and $K(k_2)$ in the expressions of bond orders p_{12}, p_{23}, p_{14}, p_{45}, p_{27}, p_{25} and p_{36} for PP2. The expression of energy per π-electron $\bar{\varepsilon}_k$ is also shown

p_{12}	$\frac{1}{a}[G_1$	G_2	G_3	$G_4]$
p_{23}	$\frac{1}{a}[WG_1$	$-WG_2$	$-RG_3$	$RG_4]$
p_{14}	$\frac{1}{a}[RG_1$	$-RG_2$	$-WG_3$	$WG_4]$
p_{45}	G_1	G_2	G_3	G_4
p_{27}	W^2G_1	W^2G_2	R^2G_3	R^2G_4
p_{25}	WG_1	WG_2	$-RG_3$	$-RG_4$
p_{36}	$\frac{1}{3}[(a^2W^2-2)G_1$	$(a^2W^2+2)G_2$	$(a^2R^2-2)G_3$	$(a^2R^2+2)G_4]$

$$\bar{\varepsilon}_\pi = (W^2+1)G_1E(k_1) + (R^2+1)G_3E(k_2) = \tfrac{1}{2}(2ap_{12} + ap_{23} + p_{45} + p_{27})$$

$$G_2 = \frac{2a+\sqrt{5}-1}{2\pi\sqrt{5}}, \qquad G_2 = \frac{-2a+\sqrt{5}-1}{2\pi\sqrt{5}},$$

$$G_3 = \frac{2a+\sqrt{5}+1}{2\pi\sqrt{5}}, \qquad G_4 = \frac{-2a+\sqrt{5}+1}{2\pi\sqrt{5}},$$

$$W = \frac{\sqrt{5}+1}{2}, \qquad R = \frac{\sqrt{5}-1}{2}$$

$$k_1 = \frac{2\sqrt{2a(\sqrt{5}+1)}}{(\sqrt{5}+1)a+2}, \qquad k_2 = \frac{2\sqrt{2a(\sqrt{5}-1)}}{(\sqrt{5}-1)a+2}.$$

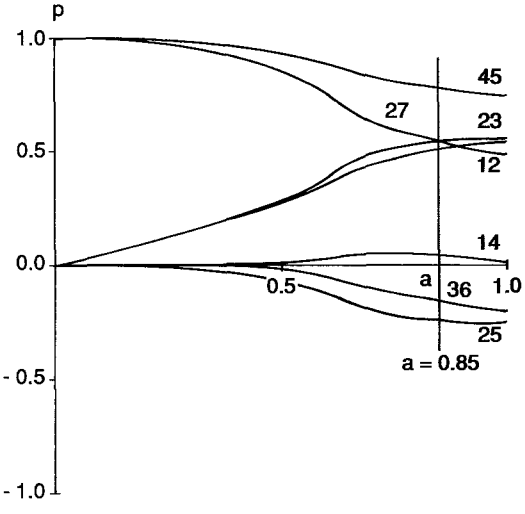

Fig. 9. Curves of the bond orders as a function of parameter a for PP2

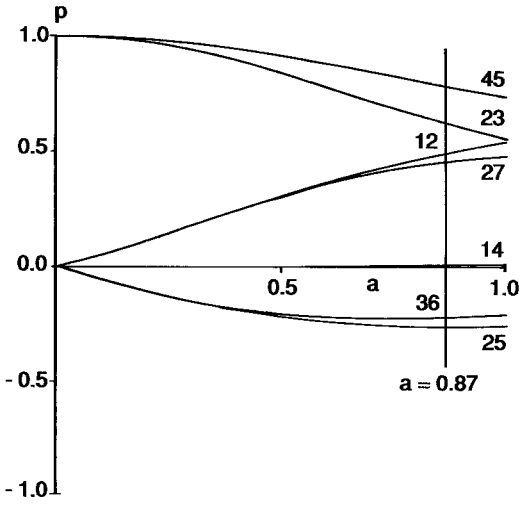

Fig. 10. a-Dependency of the bond orders of PP3. For the values at $a = 0.87$, the bond orders agree quite well with those obtained by Tanaka et al. [4], by using the so-called one-dimensional tight-binding SCF-CO method

The bond orders for the bonds in PP3 were calculated numerically as plotted in Fig. 10, as their analytical expressions could not be obtained. Since there is no crossing point in Fig. 10, and the relative values of bond orders are consistent with the bond alternation pattern in Fig. 2, the PP3 pattern seems to be the most plausible structure for polyphenanthrene in view of the bond orders.

Comparison with more sophisticated calculation can also be performed as described for polyacene. Tanaka et al. [4] give their calculated values of bond orders, p_{45}, p_{12}, p_{27}, and p_{23}, to be 0.785, 0.502, 0.463, and 0.615, respectively, by the SCF-CO method. All these bond orders are found to have no large difference from our results, 0.784, 0.499, 0.456, and 0.635, obtained for PP3 with a single parameter a to be 0.87. Thus it is worthy of notice that if the bond alternation is properly taken into consideration, the Hückel MO calculation can reproduce satisfactorily well with the results obtained by the calculation of higher quality.

The energy per π-electron for PP3 can be expressed as:

$$\bar{\varepsilon}_\pi = \frac{1}{2\sqrt{2}\pi} * \left[\int_0^\pi \sqrt{3a^2 + 2 + 2a\cos k\theta + \sqrt{4a^2(4a+1)\cos^2 k\theta + 4a^2(3a+2)\cos k\theta + a^2(5a^2 - 8a + 8)}}\, dk\,\theta + \int_0^\pi \sqrt{3a^2 + 2 + 2a\cos k\theta - \sqrt{4a^2(4a+1)\cos^2 k\theta + 4a^2(3a+2)\cos k\theta + a^2(5a^2 - 8a + 8)}}\, dk\,\theta \right]. \tag{27}$$

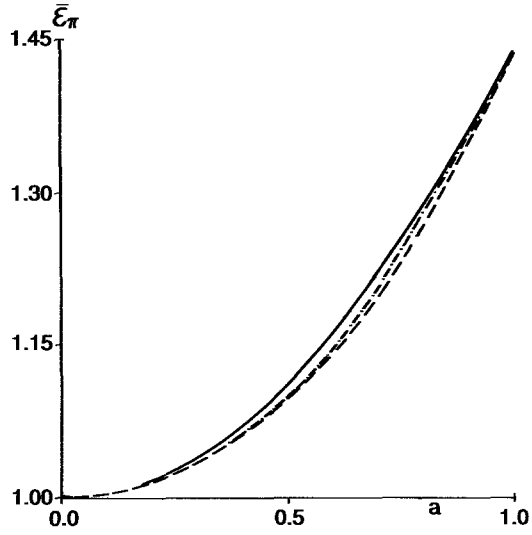

Fig. 11. Curves of energy per π-electron $\bar{\varepsilon}_\pi$ as a function of parameter a. The *dotted line*, *dashed line with dots*, and *solid line* are those for PP1, PP2 and PP3

However, the integral is too difficult to be analytically treated, an attempt was made to obtain its numerical results, as shown in Fig. 11 by the solid line. The energy per π-electron $\bar{\varepsilon}_\pi$ for PP1 and PP2 is also depicted by the dotted line and dashed line with dots, respectively. Among the three bond alternation isomers considered, PP3 is the most stable, while PP1 the most unstable.

Figure 12 shows the band structures of PP1, PP2 and PP3 versus the parameter a. These band structures are obtained from the analytical expressions of x. For example, for PP1 we can easily obtain four independent sets of the x solution from Eq. (23) as:

$$x = \pm\sqrt{\frac{(3a^2+2+2a^2\cos k\theta) \pm a(2\cos k\theta+1)\sqrt{a^2+4}}{2}}. \tag{28}$$

Since $k\theta = 2\pi k/N$, with $k = 1, 2, \ldots, N$, each of the four x roots expresses the energy levels of N states. For an infinitely large network, since $N \to \infty$, these energy levels converge to form bands. For PP1 and PP2 the lower and upper boundaries of the bands corresponding to the x solutions are obtained with

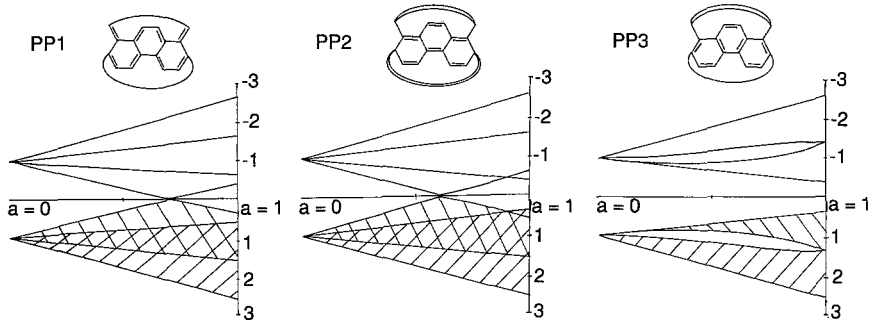

Fig. 12. Band structures of PP1, PP2 and PP2 against parameter a

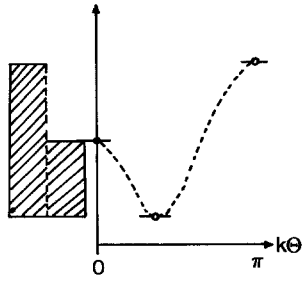

Fig. 13. Schematic diagram of self overlapping of the band

$\cos k\theta = -1$ and $+1$, respectively. Although there is a possibility of the so-called self overlapping of bands [23] as shown in Fig. 13, the boundary of the band cannot always be determined by the x solutions at the Brillouin zone boundary, namely, the x solutions in $\cos k\theta = \pm 1$, we can prove that there is no self overlapping of bands in the case of PP1 and PP2. However, for the two middle band boundaries of PP3, x is not a monotonic function of $k\theta$. From Eq. (26), we obtain:

$$\cos k\theta = \frac{x^2 + a - 1 \pm \sqrt{(4a+1)x^4 - 2x^2(6a^3 + 3a + 1) + (1+a)^2(4a^3+1)}}{-4a^2}. \tag{29}$$

It is obvious that, apart from the condition of $|\cos k\theta| \leqslant 1$, there is also a condition that the value in the square root must be positive; hence we know that in the region of:

$$\sqrt{\frac{6a^3 + 3a + 1 - 2a\sqrt{a(1-a^2)(3a+1)}}{4a+1}} < x < \sqrt{\frac{6a^3 + 3a + 1 + 2a\sqrt{a(1-a^2)(3a+1)}}{4a+1}} \tag{30}$$

no states exist, and this determines the two middle boundaries.

For PP1 and PP2, the HOMO-LUMO gap is zero when a is $1/\sqrt{2}$ ($= 0.707$) and $(\sqrt{5}-1)/2$ ($=0.618$), respectively. On the other hand, for PP3 the HOMO-LUMO gap never becomes zero, and the larger the parameter a, the larger the gap.

5. MO-benzene character

Several benzene characters have been proposed to describe the degree of local aromaticity in the component hexagons [24, 25]. Polansky and Derflinger [26] defined the MO-benzene character r_L for alternant hydrocarbons by using the Coulson bond orders as:

$$r_L = \frac{1}{2} + \frac{1}{18}\left(2\sum^{L} p_{\text{ortho}} - \sum^{L} p_{\text{para}}\right). \tag{31}$$

In Ref. [27], Aida and Hosoya defined and normalized MO-benzene character as:

$$\begin{aligned}\bar{r}_L &= 6r_L - 5 \\ &= \frac{1}{3}\left(2\sum^{L} p_{\text{ortho}} - \sum^{L} p_{\text{para}}\right) - 2,\end{aligned} \tag{32}$$

making $\bar{r}_L$ vary from 0 for three isolated double bonds to 1.0 for benzene.

Since we have obtained the analytical solutions of all the bond orders for polyphenanthrene PP1 and PP2, the normalized MO-benzene character can easily be derived as:

$$\bar{r}_L = \tfrac{2}{3}(2p_{12} + 2p_{23} + p_{27} + p_{45}) - \tfrac{1}{3}(2p_{25} + p_{36}) - 2. \tag{33}$$

By substituting the expressions of the bond orders, the analytical expressions of $\bar{r}_L$ for PP1 can be obtained as:

$$\begin{aligned}\bar{r}_L = \tfrac{1}{18}\{&[(17a-6)\sqrt{a^2+4} + (21a^2+18a+22)]A_1E(k_1) \\ &- [(7a+6)\sqrt{a^2+4} + (11a^2+30a-22)]B_1K(k_1) \\ &- [(17a-6)\sqrt{a^2+4} - (21a^2+18a+22)]A_2E(k_2) \\ &+ [(7a+6)\sqrt{a^2+4} - (11a^2+30a-22)]B_2K(k_2)\} - 2.\end{aligned} \tag{34}$$

Similarly, the analytical expression of $\bar{r}_L$ for PP2 is obtained as:

$$\begin{aligned}\bar{r}_L = \frac{3+\sqrt{5}}{18a}\{&[12 + 7(3-5\sqrt{5})a - a^3]G_1E(k_1) \\ &- [12 - 5(3-\sqrt{5})a + a^3]G_2K(k_1)\} \\ + \frac{3-\sqrt{5}}{18a}\{&[12 + 7(3+\sqrt{5})a - a^3]G_3E(k_2) \\ &- [12 - 5(3+\sqrt{5})a + a^3]G_4K(k_2)\} - 2.\end{aligned} \tag{35}$$

For PP3, since we only have the numerical results of each bond, the analytical expression of $\bar{r}_L$ cannot be obtained, the numerical results are plotted in Fig. 14. The curves of $\bar{r}_L$ as a function of parameter a for PP1 and PP2 are also plotted. It is shown that the component hexagon of PP3 has the largest benzene property in all the range of $0 \leqslant a \leqslant 1$. The curve of PP3 has a maximum when a is about 0.7.

According to Ref. [27] of the PPP type calculation, if the network of polyphenanthene is large enough, (>ca. 25 rings), the value of the benzene character $\bar{r}_L$ of the central ring converges to 0.56947. This value is found to correspond with our result of PP3 with $a = 0.94$. However, for PP1 and PP2, in all the range of $0 \leqslant a \leqslant 1$, $\bar{r}_L$ of HMO calculation never gets larger than 0.52630, and therefore there is no value compatible with that of PPP. In this respect, PP3 is also considered to be the best candidate among the bond alternation isomers.

The benzene characters $\bar{r}_L$ for PA isomers are also calculated as shown in Fig. 15. When a is larger than about 0.9, $\bar{r}_L$ for the three isomers do not have large differences, while in the range of $0 \leqslant a \leqslant 0.9$, PA3 has the largest $\bar{r}_L$.

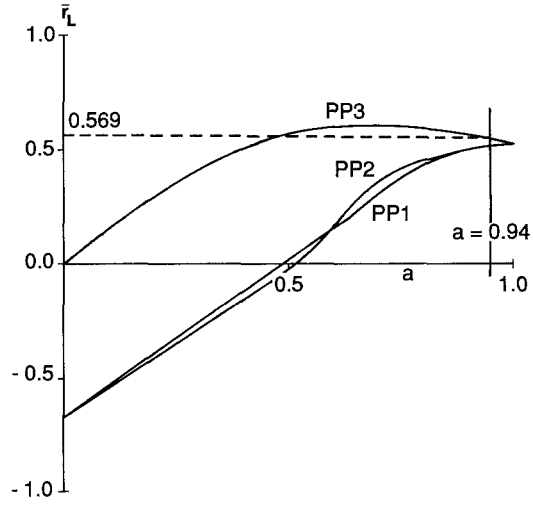

Fig. 14. Curves of the benzene characters versus parameter a for PP1, PP2 and PP3

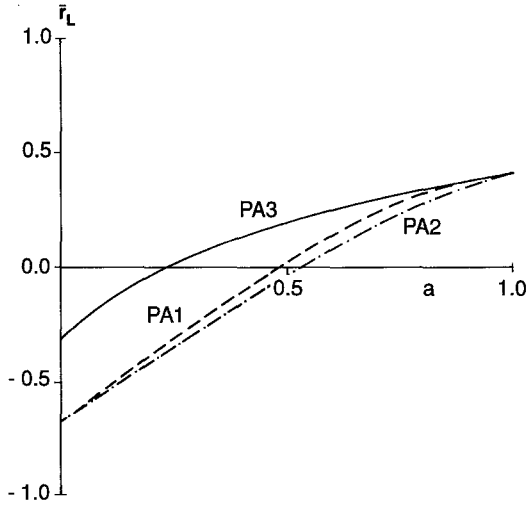

Fig 15. Curves of the benzene characters versus parameter a for PA1, PA2 and PA3

6. Conclusion

Analytical expressions of various HMO properties are obtained for infinitely large polyacene and polyphenanthrene with bond alternation. From these results, we can get some basic information about the π-electronic structures of these networks. For polyphenanthrene, PP3 structure is found to be the most stable and the most plausible isomers from the analysis of the bond orders and the benzene character. For polyacene, the effect of bond alternation to the bond order and relative stability can be derived.

It is shown that if the bond alternation is properly taken into consideration in the HMO calculation of large periodic π-electronic networks, we can get rather reliable results as compatible with more sophisticated methods, such as PPP and SCF-CO calculations.

Acknowledgement. This work was supported by the Grant-in-Aid for Scientific Research from the Ministry of Education, Science and Culture, Japanese Government.

References

1. Salem L, Longuet-Higgins HC (1960) Proc Roy Soc A255:435
2. Whangbo MH, Hoffmann R, Woodward RB (1979) Proc R Soc Lond A366:23
3. Mishima A, Kimura M (1985) Synthetic Metals 11:25
4. Tanaka K, Ohzeki K, Nankai S, Yamabe T, Shirakawa H (1983) J Phys Chem Solids 44:1069
5. Kivelson S, Chapman OL (1983) Phys Rev B 28:7236
6. Schaad LJ, Hess BA Jr, Nation JB, Trinajstic N, Gutman I (1979) Croat Chem Acta 52:233
7. Heilbronner E (1954) Helv Chim Acta 37:921
8. Graovac A, Polansky OE, Tyutyulkov NN (1983) Croat Chem Acta 56:325
9. Kertesz M, Lee YS, Stewart JJP (1989) Int J Quantum Chem 35:305
10. Boon MR (1971) Theoret Chim Acta 23:109
11. Kertesz M, Hoffmann R (1983) Solid State Commun 47:97
12. Tanaka K, Koike T, Yamabe T, Yamauchi J, Deguchi Y, Yata S (1987) Phys Rev B 35:8368
13. Ozaki M, Ikeda Y, Nagoya I (1987) Synth Metals 18:485
14. Kimura M, Kawabe H, Nishikawa K, Aono S (1986) J Chem Phys 85:3090
15. Aono S, Nishikawa K, Kimura M, Kawabe H (1987) Synth Metals 17:167
16. Unpublished results of our group
17. Coulson CA, Longuet-Higgins HC (1947) Proc Roy Soc London A191:39
18. Hosoya H, Tsuchiya A (1989) J Mol Struct (Theochem) 185:123
19. Gao YD, Hosoya H (1990) J Mol Struct (Theochem) 206:153
20. Hosoya H, Aida M, Kumagai R, Watanabe K (1987) J Comput Chem 8:358
21. Abramowitz M, Stegun IA (eds) (1964) Handbook of Mathematical Functions. Natl Bur Stand Washington, D.C.
22. Ledermann W (1944) Proc Roy Soc A182:362
23. Polansky OE, Tyutyulkov NN (1976) Match 3:149
24. Sakurai K, Kitaura K, Nishimoto K (1986) Theor Chim Acta 69:23
25. Hosoya H, Hosoi K (1975) Theor Chim Acta 38:37
26. Polansky OE, Derflinger G (1967) Int J Quantum Chem 1:379
27. Aida M, Hosoya H (1980) Tetrahedron 36:1317